Photonic Anisotropic Magnetoresistance in Dense Co Particle Ensembles

K. J. Chau and A. Y. Elezzabi

Ultrafast Photonics and Nano-Optics Laboratory, Department of Electrical and Computer Engineering, University of Alberta, Edmonton, Alberta, Canada T6G 2V4

(Received 10 June 2005; published 24 January 2006)

In this Letter, we experimentally show that the amplitude and arrival time of the terahertz optical transmission through dense ensembles of subwavelength-size ferromagnetic particles is strongly dependent on the orientation of an externally applied magnetic field. The attenuation and delay have the same magnetic field orientation dependence as the electrical anisotropic magnetoresistance inherent to bulk ferromagnetic metals. We envision the application of this magnetic effect in terahertz photonic devices.

DOI: 10.1103/PhysRevLett.96.033903 PACS numbers: 42.25.Dd, 73.20.Jc, 73.20.Mf, 75.30.Gw

Magnetoresistance, the magnetically induced resistance change in ferromagnetic metals, is the backbone of advanced technologies such as spintronics, magnetic sensors, recording heads, and memories [1–3]. While magnetoresistance has been studied extensively in relation to electrical transport, the incorporation of magnetoresistive effects into photonic systems could potentially lead to a plethora of next generation devices [2]. A magnetoresistance effect associated with light was demonstrated in paramagnetic dielectric scatterers [4,5]. A new route towards observing photonic magnetoresistance is via ferromagnetic metallic scattering media. In particular, when light is coupled into charge oscillations on metallic surfaces (surface plasmons), the optical properties of the supporting medium can be influenced via the mediating charge oscillations. In the scenario where the conduction electron oscillations, which behave as localized currents, are confined to a ferromagnetic metal surface, magnetically dependent spin-orbit scattering responsible for the anisotropic magnetoresistance effect [6–8] will map onto an analogous photonic anisotropy. Like electronic conduction, light propagation in such plasmonic systems will exhibit a strong dependence on the orientation of a magnetic field.

Recently, it was shown that ensembles of metallic microparticles exhibit high terahertz (THz) electromagnetic transparency due to coherent near-field coupling of surface plasmons across the medium [9–11]. As electromagnetic transmission in these dense metallic particle collections is mediated by coupled surface plasmon oscillations, such media exhibit optical properties that are sensitive to the particles' electrical and magnetic characteristics. In this Letter, we investigate THz plasmon-mediated transmission through dense, random ensembles of subwavelength ferromagnetic Co particles above the critical metal fraction [12]. Plasmon oscillations at the particles' surfaces behave as localized currents that are influenced by the resistivity of the metallic medium. We find that the Co particle ensembles show strong magnetically dependent transmission modulation not present in nonmagnetic particles. The large transmissivity modulation arises from anisotropic magnetoresistivity inherent to the ferromagnetic metal. Our experimental results are presented in conjunction with a description of plasmon modulation due to anisotropic magnetoresistivity.

To observe photonic magnetoresistance, we employ THz time domain spectroscopy [10]. The sample is $>99.7\%$ pure Co, consisting of randomly shaped, polydisperse particles, with a mean dimension of $\alpha = 74$ μm and a volume packing fraction of 0.51. The Co particles are magnetized using a biasing magnetic field B. Far infrared radiation is utilized to explore electromagnetic interaction in a regime where the wavelength $\lambda \gg \alpha$. Single-cycle, broadband (1 THz bandwidth), 1 ps wide THz pulses are generated from a semi-insulating GaAs photoconductive switch illuminated with 20 fs, 800 nm laser pulses. The THz pulse is directed upon a polystyrene cell housing the Co particles with sample length L, ranging from 2 to 9 mm. The on-axis transmitted electric field is coherently detected in a $\langle 111 \rangle$ ZnSe electro-optic (EO) crystal [9].

The THz electric field pulse $\boldsymbol{E}_{\mathrm{THz}}$ incident on the Co particles excites localized conduction electron oscillations within the skin depth of the particle surface. The current associated with the charge oscillations can be described by $\boldsymbol{j}_p = \boldsymbol{E}_{\mathrm{total}}/\rho_{\mathrm{eff}}(B, \theta)$, where $\boldsymbol{E}_{\mathrm{total}} = \boldsymbol{E}_{\mathrm{THz}} + \boldsymbol{E}_{\mathrm{depol}}$ is the total surface electric field consisting of contributions from $\boldsymbol{E}_{\mathrm{THz}}$ and the depolarization electric field $\boldsymbol{E}_{\mathrm{depol}}$ from the induced charges. The medium is characterized by an effective resistivity $\rho_{\mathrm{eff}}(B, \theta) = \rho_o + \rho_{\mathrm{Lorentz}}(B, \theta) + \rho_{\mathrm{AMR}}(B, \theta)$, where ρ_o is the nonmagnetic background resistivity, $\rho_{\mathrm{Lorentz}}(B, \theta)$ is the magnetoresistivity arising from Lorentz force, $\rho_{\mathrm{AMR}}(B, \theta)$ is the magnetoresistivity due to the anisotropic magnetoresistance (AMR) effect, and θ is the angle between the current and the magnetization direction. In all metals, $\rho_{\mathrm{Lorentz}}(B, \theta)$ is present as a small magnetoresistivity modulation proportional to the Lorentz force $-e\boldsymbol{v} \times \boldsymbol{B}$, where e and $\boldsymbol{v}$ are the electron charge and velocity, respectively. In ferromagnetic metals, $\rho_{\mathrm{AMR}}(B, \theta)$ is a significantly larger magnetoresistivity effect where the resistivity is maximum (minimum) when the electron velocity is parallel (perpendicular) to the magnetization. The dependence of $\rho_{\mathrm{AMR}}(B, \theta)$ on θ is given by $\rho_{\mathrm{AMR}}(\theta) = \rho_\perp + (\rho_\parallel - \rho_\perp)\cos^2\theta$ [13], where

$\rho_\perp$ and $\rho_\parallel$ are the resistivities when the magnetization is perpendicular and parallel to the current direction, respectively. AMR originates from scattering anisotropy due to spin-orbit interaction [7]. Stronger scattering is expected for electrons traveling parallel to the magnetization, causing $\rho_\parallel > \rho_\perp$. By means of plasmonic propagation, changes in $\rho_{\text{eff}}(B, \theta)$ within the skin depth of the particle surface via $\rho_{\text{Lorentz}}(B, \theta)$ and/or $\rho_{\text{AMR}}(B, \theta)$ cause a magnetically dependent transmissivity modulation.

By magnetically varying the resistivity of the Co particles, THz light transmission through the ensembles is influenced through $\rho_{\text{Lorentz}}(B, \theta)$, $\rho_{\text{AMR}}(B, \theta)$, or both. As shown in Fig. 1, the time domain characteristics of the experimental THz transmission through the Co sample reveal several magnetic effects. The most remarkable observation is that the THz pulse arrival time T (measured at the first peak of the transmitted pulse) depends on the orientation of the biasing B field ($B = 0.18$ T) relative to the incident pulse polarization. This observation is accompanied by simultaneous transmission attenuation exhibiting a similar B-orientation dependence. As shown in Figs. 1(b)–1(f), the magnetic arrival delay and attenuation increase with increasing L. Evidently, the optical properties of the Co sample are highly dependent on the angle between the THz pulse polarization and the sample magnetization. Arrival delay ΔT and attenuation are observed only with the application of $B_\parallel$ parallel to the incident THz pulse polarization; however, as shown in Fig. 1(g), no measurable ΔT and attenuation occur for the configuration $B_\perp$ perpendicular to the incident polarization. It should be noted that identical behavior observed using Co embedded in solid paraffin shows that the delay and attenuation are not caused by spurious mechanical effects such as particle physical rearrangement in the $B_\parallel = 0.18$ T field (not shown). The attenuation and delay have a similar B-orientation dependence as AMR inherent to bulk ferromagnetic metals [7]. The increased temporal delay and attenuation when a $B_\parallel$ field is applied indicate a decreased relaxation time, which can be equivalently interpreted as an increase in $\rho_{\text{AMR}}(B, \theta)$ of the medium. In contrast, the insignificant attenuation and delay observed in a $B_\perp$ field show that $\rho_{\text{Lorentz}}(B, \theta)$ is negligible.

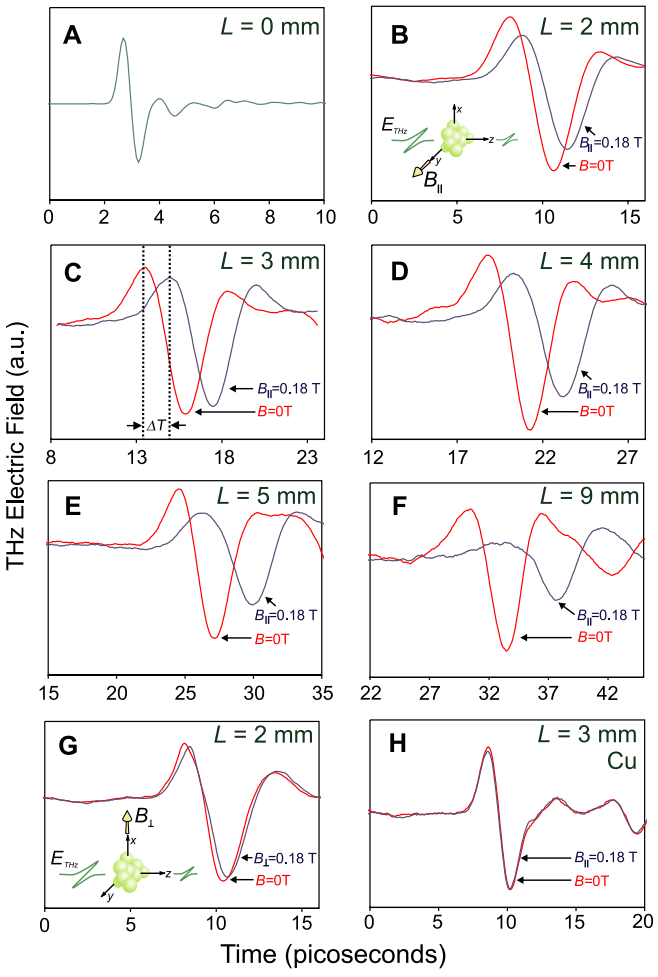

FIG. 1 (color online). Time domain transmitted THz waveforms when (a) $L = 0$ mm, (b) $L = 2$ mm, (c) $L = 3$ mm, (d) $L = 4$ mm, (e) $L = 5$ mm, and (f) $L = 9$ mm using the B configuration shown in the inset in (b). (g) The time domain THz transmission through a 2 mm thick Co sample using the B configuration shown in its inset. Transmission measurements made through a 3 mm thick sample of 50 μm Cu particles are illustrated in (h) for $B_\parallel = 0.18$ T and $B = 0$ configurations.

By varying the $B_\parallel$ field from 0 to 0.15 T, we find that the magnetically induced delay for a $L = 3$ mm sample grows linearly from 0 to 1.2 ps, and in the range of 0.15–0.25 T, the delay begins to saturate [Fig. 2(a)]. Employing $B_\parallel = 0.18$ T (corresponding to the onset of delay saturation), we observe that ΔT increases linearly with L with a retardation coefficient of $\Delta T/L = 0.57 \pm 0.01$ ps/mm [Fig. 2(b)], indicating that the phenomenon is a cumulative effect proportional to the number of Co particles across the sample. To quantify this photonic anisotropy, we introduce the photonic magnetoresistance ratio PMR $= (\tau_\parallel - \tau_0)/\tau_0$, where $\tau_\parallel$ and τ_0 are the temporal delays for $B_\parallel = 0.18$ T and $B = 0$, respectively. We obtain PMR $= 15 \pm 2\%$ for all thickness values. Further evidence is drawn from comparative transmission measurements through an ensemble of ~ 70 μm Cu particles with the application of $B_\parallel = 0.18$ T. As Cu is nonmagnetic, we observe no measurable magnetically dependent delay, evident in Fig. 1(h). In addition, for the Co particles, we do not observe B-polarity-dependent transverse plasmon scattering effects in the transmission amplitude, delay, or spatial distribution [14,15].

Anisotropic transmission modulation in the metallic particles arises directly from the θ-dependent electrical magnetoresistivity of the ferromagnetic metal. This can be understood by describing the vector plasmonic response of a single Co particle. As the size scale of the particles' roughness (~ 1 μm) relative to the central wavelength obey Rayleigh's criterion for smooth surfaces, the particle is approximated to be a smooth sphere [16]. For $\alpha \ll \lambda$, the incident THz pulse can be described as a homogeneous

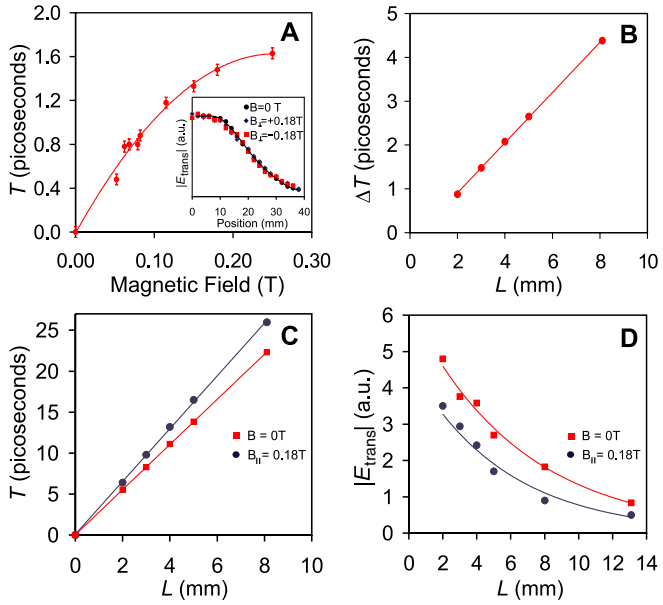

FIG. 2 (color online). (a) The transmission arrival time versus magnetic field through a $L = 3$ mm Co sample. The inset in (a) depicts the integrated spatial profile along the polarization axis of the THz transmission through a Co sample for $B = 0$ T, $B_\perp = +0.18$ T, and $B_\perp = -0.18$ T. The integrated spatial profile of the transmission shows no B-polarity-dependent effects. (b) The relative delay versus sample thickness for the $B_\parallel = 0.18$ T configuration with respect to $B = 0$. (c) Arrival time and (d) peak-to-peak electric field amplitude $|E_{\text{trans}}|$ of the transmitted THz pulse for $B_\parallel = 0.18$ T and $B = 0$ T versus sample thickness. The arrival times correspond to velocities of $v_{g,\parallel} = 0.51 \pm 0.01$ c and $v_{g,0} = 0.55 \pm 0.01$ c for $B_\parallel = 0.18$ T and $B = 0$ T, respectively.

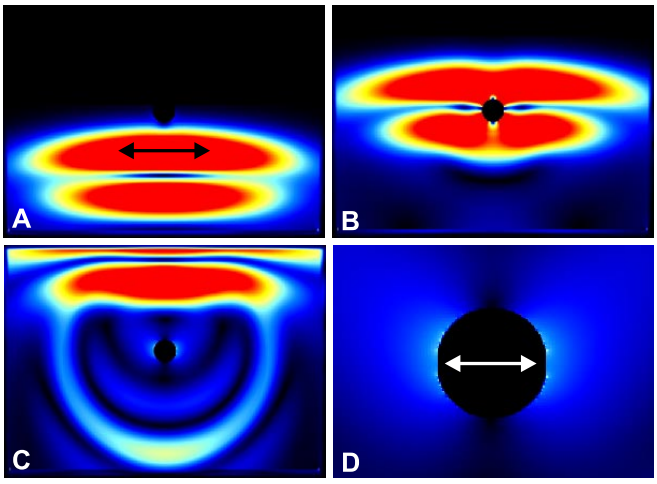

FIG. 3 (color online). Electric field amplitude images of a finite difference time domain simulation of single-cycle THz pulse excitation of a 70 μm diameter Co particle at various times. Experimental data from Ref. [19] are used to fit the Drude permittivity $\varepsilon(\omega) = 1 - \omega_p^2/(i\Gamma\omega - \omega^2)$, where $\omega_p = 9.8 \times 10^{14}$ s^{-1} and $\Gamma = 1.0 \times 10^{13}$ s^{-1} are the plasma and damping frequencies for Co, respectively. As shown in (a), at 6.5 ps the single-cycle TM polarized THz pulse propagates towards the Co particle. At 10 ps, shown in (b), negligible THz field amplitude is present inside the particle due to the large imaginary permittivity at THz frequencies. (c) and (d) show that, after passage of the THz pulse at 15 ps, the fields near the Co particle exhibit strong dipolelike signatures associated with the surface currents at the left and right edges of the particle. The arrows in (a) and (d) depict the orientations of the THz pulse polarization and the net induced dipole in the particle, respectively. In the images, the field amplitude increases from black (0), to blue, to yellow, up to red (1).

electric field $\boldsymbol{E}_{\text{THz}} = E_{\text{THz}}(\cos\phi\hat{r} - \sin\phi\hat{\phi})$. The depolarization electric field $\boldsymbol{E}_{\text{depol}}$ of the surface charges induced by $\boldsymbol{E}_{\text{THz}}$ corresponds to that of a dipole moment $\boldsymbol{p}$ directed along $\boldsymbol{E}_{\text{THz}}$. The dipole electric field is $\boldsymbol{E}_{\text{depol}} = (p/4\pi\varepsilon_o r^3)(2\cos\phi\hat{r} + \sin\phi\hat{\phi})$ [17], where ε_o is the permittivity of free space, r is the radial distance from the particle center, and ϕ is the angle of an arbitrary direction. Cancellation of the tangential electric fields at the particle surface results in a total surface electric field $\boldsymbol{E}_{\text{total}} = \boldsymbol{E}_{\text{THz}} + \boldsymbol{E}_{\text{depol}} = E_{\text{THz}}\cos\phi\hat{r}$ oriented normal to the particle surface. Note that $\boldsymbol{E}_{\text{total}}$ is strongest along the direction of the incident field ($\phi = 0°$) and approaches zero in the orthogonal direction ($\phi = 90°$). Accordingly, surface plasmon oscillations driven by the total electric field $\boldsymbol{j}_p = \boldsymbol{E}_{\text{total}}/\rho_{\text{eff}}(B, \theta) = (E_{\text{THz}}\cos\phi\hat{r})/\rho_{\text{eff}}(B, \theta)$ are also polarized along the incident field direction. This is illustrated by finite difference time domain simulations shown in Fig. 3. In a collection of particles, the plasmon oscillations on individual particles coherently couple across the extent of the sample and at the edge, radiate into the far field. Polarization of the surface currents along the incident electric field gives rise to the observed anisotropy. The characteristic $\rho_{\text{eff}}(B, \theta)$ of the ferromagnetic particles depends strongly on the angle between the incident field polarization (coinciding with the orientation of the surface currents) relative to the magnetic field direction. Attenuation of $\boldsymbol{j}_p$ via $\rho_{\text{AMR}}(B, \theta) \gg \rho_{\text{Lorentz}}(B, \theta)$ directly results in transmission amplitude reduction and delay in a $B_\parallel$ field relative to a $B_\perp$ field. Since Cu exhibits negligible magnetoresistivity, no magnetically induced transmission modulation is observed in the Cu particles.

Polarization characterization of the experimental transmission enables further understanding of this photonic effect. Depending on the orientation φ of the EO crystal, relative to the incident THz pulse polarization, we measure different components of the transmitted electric field. The EO response of the $\langle 111 \rangle$ ZnSe crystal at $\varphi = 0°$, $60°$, and $120°$ correspond to the transmitted field component parallel to the incident polarization, while the responses at $\varphi = 30°$ and $90°$ correspond to electric field components along the perpendicular direction [18]. By measuring the electric field signal from $\varphi = 0°$ to $\varphi = 120°$, all field components are sampled. Figure 4 maps the experimentally measured transmitted electric field (through a 3 mm thick sample) as a function of the angle φ for $B = 0$, $B_\parallel$, $B_\perp$, and B_{45} at $45°$ with respect to the incident THz pulse

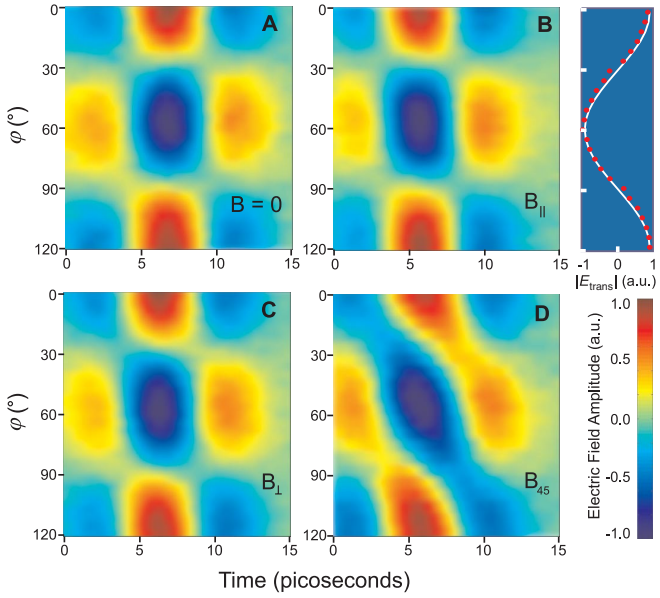

FIG. 4 (color online). Normalized THz electric field amplitude versus φ and time for (a) $B = 0$, (b) $B_{\parallel}$, (c) $B_{\perp}$, and (d) B_{45} configurations. Shown in the side panel is the peak-to-peak THz electric field amplitude versus φ for $B = 0$. The magnetic field in the $B_{\perp}$, $B_{\parallel}$, and B_{45} configurations is 0.18 T.

polarization. For $B = 0$ [Fig. 4(a)], coherent coupling across the medium preserves the incident linear polarization as evidenced by the threefold symmetry of the transmitted electric field, where maxima occur at $\varphi = 0°$, 60°, and 120° and the field is 0 at $\varphi = 30°$ and 90°. The high polarization purity suggests the absence of significant polarization-randomizing scattering events. A similar conclusion can be drawn when $B_{\parallel}$ and $B_{\perp}$ are applied [Figs. 4(b) and 4(c)], where the THz pulse propagates isotropically at velocities $v_{g,\parallel}$ and $v_{g,\perp} \approx v_{g,0}$, respectively. However, when a B_{45} field is applied, the incident THz pulse simultaneously excites charge oscillations oriented both parallel and perpendicular to B_{45} that travel across the sample at velocities of $v_{g,\parallel} = 0.51$ c and $v_{g,\perp} = 0.55$ c, respectively. Because of this anisotropy, the transmitted electric field does not preserve the incident linear polarization, and it is anticipated that the transmission contains electric field components along all EO crystal orientations. Indeed, as shown in Fig. 4(d), the temporal electric field map versus φ shows entirely different behavior from the previous cases. While the threefold symmetry of the map is still evident, field components present at $\varphi = 30°$ and 90° indicate that the polarization purity is significantly reduced, in accordance with predictions for anisotropic plasmonic propagation through the medium. Anisotropic magnetoresistance causes the dense Co particle collection to exhibit extraordinarily large THz optical birefringence. In contrast, no birefringence is observed in nonmagnetic Cu samples under the same experimental conditions.

Our experiments confirm the existence of a plasmonic counterpart of the anisotropic magnetoresistance effect, a phenomenon conventionally associated with electronic transport. With this discovery, we envision the development of hybrid photonic magnetoresistive devices.

This work was supported by the Natural Sciences and Engineering Research Council of Canada.

[1] G. A. Prinz, Science **282**, 1660 (1998).
[2] S. A. Wolf *et al.*, Science **294**, 1488 (2001).
[3] N. Spaldin, *Magnetic Materials: Fundamentals and Device Applications* (Cambridge University Press, Cambridge, England, 2003).
[4] A. Sparenberg, G. L. J. A. Rikken, and B. A. van Tiggelen, Phys. Rev. Lett. **79**, 757 (1997).
[5] D. Lacoste, F. Donatini, S. Neveu, J. A. Serughetti, and B. A. Van Tiggelen, Phys. Rev. E **62**, 3934 (2000).
[6] J. Kondo, Prog. Theor. Phys. **27**, 772 (1962).
[7] T. R. McGuire and R. I. Potter, IEEE Trans. Magn. **11**, 1018 (1975).
[8] A. Gerber *et al.*, Phys. Rev. B **55**, 6446 (1997).
[9] K. J. Chau, G. R. Dice, and A. Y. Elezzabi, Phys. Rev. Lett. **94**, 173904 (2005).
[10] K. J. Chau and A. Y. Elezzabi, Phys. Rev. B **72**, 075110 (2005).
[11] F. Miyamaru and M. Hangyo, Phys. Rev. B **71**, 165408 (2005).
[12] G. L. Carr, R. L. Henry, N. E. Russell, J. C. Garland, and D. B. Tanner, Phys. Rev. B **24**, 777 (1981).
[13] J. Velev, R. F. Sabirianov, S. S. Jaswal, and E. Y. Tsymbal, Phys. Rev. Lett. **94**, 127203 (2005).
[14] G. Düchs, G. L. J. A. Rikken, T. Grenet, and P. Wyder, Phys. Rev. Lett. **87**, 127402 (2001).
[15] In-plane surface plasmon deflection in a transverse magnetic field has been observed in thin Ag films with Co scatterers in Ref. [14]. However, we observe that the spatial distribution of the THz transmission shows no magnetically dependent deflection in the plane of the THz polarization with the application of a transverse magnetic field, ruling out plasmon magnetoscattering effects.
[16] P. Beckmann and A. Spizzichino, *The Scattering of Electromagnetic Waves from Rough Surfaces* (Pergamon, New York, 1963).
[17] J. D. Jackson, *Classical Electrodynamics* (Wiley, New York, 1999), 3rd ed., p. 147.
[18] The measured THz signal at the balanced diode detector depends on $\cos(2\varphi + \theta)$, where φ and θ correspond to the orientation of the $\langle 111 \rangle$ ZnSe crystal with respect to the incident THz polarization and the transmitted THz component, respectively. For $\theta = \varphi + 90°$, the EO response is maximum at 30° and 90°.
[19] M. A. Ordal *et al.*, Appl. Opt. **22**, 1099 (1983).